

Glycine-capped silver nanoparticles: Promising catalyst for degradation of metanil yellow dye, an adulterant in turmeric powder

Garg Ayushi and Sharma Rama*

Department of Chemistry, GLA University, Mathura, INDIA

*rama.sharma@gla.ac.in

Abstract

This research aimed to identify unauthorized food colorings in spices and explore a new method for reducing these harmful substances using silver nanoparticles. Spices, known for their strong flavors and aromas, enhance the taste of many foods and beverages. However, the issue of spice adulteration poses serious health risks, making the detection of harmful contaminants essential. Glycine-capped silver nanoparticles (Gly-AgNPs) showed significant promise, effectively photo-catalyzing the breakdown of metanil yellow dye, a banned food coloring. To assess real-world implications, four turmeric powder samples were collected from local markets in Agra, specifically testing for metanil yellow.

The results were concerning: two of the four samples contained metanil yellow dye, indicating a troubling prevalence of adulteration. Gly-AgNPs proved to be highly effective catalysts, reducing the dye concentration by 89% within 120 minutes under optimized conditions. This research highlights the potential of glycine-capped silver nanoparticles as effective agents for degrading toxic dyes, suggesting significant applications in food safety and environmental cleanup.

Keywords: Glycine, silver nanoparticles, degradation, metanil yellow dye, turmeric.

Introduction

Spices are dried parts of plants like seeds, fruits, roots, bark and buds, but not leaves¹⁰. They enhance the taste and appearance of meals, making cooking more enjoyable. Spices also help to preserve food and to provide health benefits, making them valuable in our kitchens and in

traditional medicine. The spice market continues to thrive because of the unique flavors and aromas they provide. However, be cautious of adulteration, where sellers add harmful substances to spices⁵, reducing their quality and posing health risks. Common adulterants include sand, dirt, artificial colors, chalk powder and lead chromate. It is essential to keep spices pure for our health and to protect the rich flavors and traditions they represent.

Research shows that many food samples are tainted with non-permitted colors or allowed colorants exceeding established thresholds¹⁷. Among the most commonly utilized non-permitted colorants is metanil yellow (MY), a vivid yellow azo dye synthesized from diazotized metanilic acid and diphenylamine^{9,11}, as shown in fig. 1. Although MY is primarily intended for industrial applications such as dyeing wool, nylon, silk, paper, ink, aluminum and detergent, its use in the culinary world, particularly in spices like turmeric, has been observed. This practice is often aimed at enhancing the golden color of the spice, making it more visually appealing on grocery shelves². Extensive research has revealed that this chemical can unleash a cascade of severe toxic effects on various systems within the body, even when ingested in small quantities over prolonged periods^{7,14}.

Moreover, the chemical poses grave threats to reproductive health, having detrimental impacts on both the ovaries and testes¹⁸, which could compromise fertility and overall reproductive well-being. This transformation raises alarm about the potential long-term effects on health. One particularly alarming consequence of exposure to MY is the induction of toxic methemoglobinemia, which impairs the blood's ability to transport oxygen.¹⁶ In light of these issues, the present study has been designed to detect and minimize the presence of metanil yellow in turmeric samples. These samples are collected from various local markets in Agra to ensure the purity and safety of this essential spice.

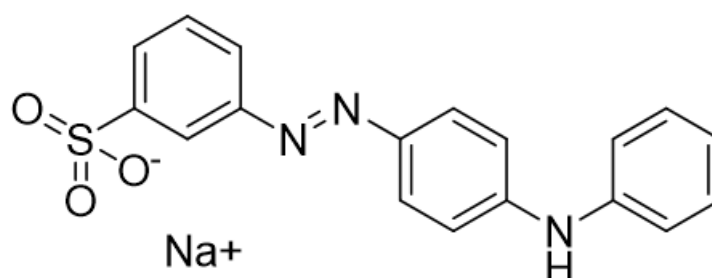


Fig. 1: Structure of metanil yellow dye

Numerous conventional methods grounded in physical and chemical principles are available for addressing the issue of dye contamination in various environments. However, the practical application of these approaches is frequently constrained by several factors including the high cost of necessary chemicals and equipment, intricate procedural steps and the potential for producing secondary pollutants. Alarmingly, some of these secondary pollutants may be more toxic than the original contaminants themselves^{13,25}. Given these challenges, advanced oxidation processes (AOP) are increasingly proposed as viable solutions to mitigate these limitations.

Among AOPs, nanoparticle (NP)-mediated processes stand out due to their ability to generate reactive oxygen species (ROS) upon exposure to light, whether visible, ultraviolet (UV), or both. These processes serve as highly effective photocatalysts for the degradation of dyes, transforming them into less harmful substances^{1,3,8,28}. Nonetheless, it is essential to note that many NP-based photocatalysts have a narrow operating range within the solar spectrum. For example, titanium dioxide (TiO₂) nanoparticles are efficient photocatalysts only when illuminated by UV light. In contrast, silver nanoparticles (AgNPs) are recognized for their versatility, as they can harness UV and visible light energy, positioning them as an attractive option for photocatalytic treatment¹².

A variety of physical and chemical methods have been used to synthesize AgNPs, often involving harmful and costly agents^{15,31}. This raises concerns about toxic by-products and the need for sustainable practices²¹⁻²³. Consequently, there is a push for eco-friendly, cost-effective methods, with green synthesis using biomolecules like proteins and vitamins as natural reducing agents emerging as a viable option^{24,29}. A straightforward method utilizing glycine amino acids has been proposed to synthesize stable AgNPs, which can be evaluated for their photocatalytic effectiveness in dye degradation. This study uses chemical analysis and degradation studies to detect and reduce metanil yellow, an adulterant in turmeric.

Material and Methods

We carefully selected standard color samples from CDH for our experimental research, ensuring that each item suited our analytical needs. Among these samples was metanil yellow, a synthetic dye known for its brilliant hue, alongside a clear solution of ethanol, which serves both as a solvent and a

reactant in various chemical processes. We also obtained concentrated hydrochloric acid, a strong acid widely used in labs for pH adjustments and reactions and crystalline silver nitrate, often utilized in colorimetric assays and photochemical applications.

Additionally, we included glycine, an amino acid that plays a critical role in biochemical reactions and sodium borohydride, a reducing agent commonly employed in organic synthesis. To complement our chemical samples, we thoroughly explored the local market in Agra, where we aimed to gather a diverse array of turmeric powder. This careful selection process allowed us to analyze the differences in quality, color intensity and other properties of turmeric sourced from different vendors (Fig. 2).

Testing method for Metanil Yellow adulteration in turmeric: In a typical analytical experiment to detect potential adulteration in turmeric, approximately 0.1 gram of the turmeric sample was meticulously weighed using a calibrated analytical balance. This precise measurement was then carefully transferred into a clean, dry test tube to prevent any contamination that could affect the results. To aid in the dissolution of the turmeric, approximately 1 milliliter of distilled water was added slowly, ensuring that the sample was thoroughly mixed to create a homogeneous solution. Following the preparation of this mixture, a critical step involved the addition of hydrochloric acid (HCl).

Specifically, 5 to 10 drops of 1N hydrochloric acid were introduced into the solution. This addition catalyzed a noticeable chemical reaction, resulting in an immediate color change that was closely monitored throughout the process. A distinct pink hue in the mixture was an essential indicator of metanil yellow, a synthetic dye commonly used as an adulterant in turmeric. To further investigate the samples and to support the initial findings, the spectra of pure metanil yellow were recorded. This was done using absolute ethanol as a solvent, providing a suitable spectral analysis medium. The recorded spectra of the pure dye were then compared with those obtained from the adulterated turmeric samples. This comparative analysis enabled a comprehensive evaluation of the results, helping to confirm the presence and concentration of any adulterants within the turmeric sample.

Synthesis of Silver Nanoparticles: Glycine-capped silver nanoparticles (Gly-AgNPs) were synthesized using a one-pot procedure, as depicted in fig. 3.



Fig. 2: Turmeric samples collected from different areas

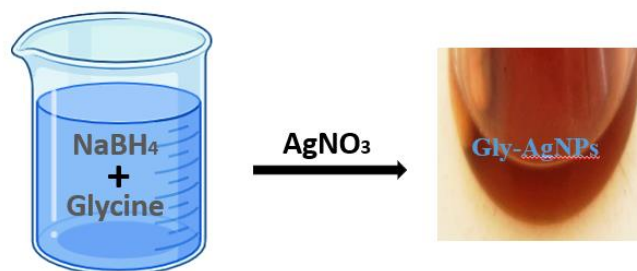


Fig. 3: One-pot synthesis of Gly-AgNPs

To begin, a 100 mM solution of glycine was prepared by carefully dissolving the amino acid in triple-distilled water, ensuring maximum purity. Next, 20 milliliters of this clear solution were transferred into a separate beaker, where it was placed on a magnetic stirrer to achieve a uniform mixture. To initiate the nanoparticle formation, 10 milliliters of freshly prepared 4 mM ice-cold sodium borohydride (NaBH_4) solution were added dropwise to the stirring amino acid solution. The dropwise addition was crucial, allowing for controlled and steady reduction.

Once the NaBH_4 was fully integrated, dropwise, 10 milliliters of a 1 mM aqueous silver nitrate (AgNO_3) solution were introduced into the mixture. This step triggered a fascinating transformation, as the silver ions in AgNO_3 were rapidly reduced to form silver nanoparticles. This was visually manifested by the solution's immediate and striking color change from colorless to a rich, dark brown hue, indicating successful nanoparticle formation. The mixture was then stirred continuously for 5 to 6 hours, allowing optimal interaction between the components and ensuring the formation of well-dispersed nanoparticles.

After this stirring period, the resulting colloidal solution of silver nanoparticles was subjected to centrifugation to separate the nanoparticles from the solution. The nanoparticles were washed with double-distilled water to eliminate any uncoordinated amino acids. Finally, the silver nanoparticles were carefully dried and characterized to assess their properties and to confirm their formation.

Photocatalytic Experiment: In this experiment, we prepared an aqueous solution of 1 gm turmeric sample mixed with a weighed quantity of metanil yellow. We prepared 50 mL of this solution with a metanil yellow concentration of 0.04 mg. The solution was gently stirred at room temperature and kept in the dark for 30 minutes, allowing it to reach a state of equilibrium. Once the solution was stabilized, we carefully added 10 mg of the synthesized silver nanoparticles (AgNPs) at 70°C . The mixture was then subjected to magnetic stirring for an additional 20 minutes, ensuring thorough dispersion of the nanoparticles throughout the solution.

We adjusted the solution using either 0.1 M sulfuric acid (H_2SO_4) or 0.1 M sodium hydroxide (NaOH) to maintain the pH 7. Following this adjustment, the solution was exposed

directly to sunlight, initiating the photocatalytic reaction. At designated time intervals (10 minutes) during the sunlight exposure, we collected a 2 mL aliquot from the analysis solution. The photocatalytic degradation was observed by UV-Vis. spectrophotometer at regular time intervals.

Characterization: The synthesis of silver nanoparticles (AgNPs) was carefully monitored by observing the distinct color changes in the solution, which signaled the formation of these nanoparticles. Their absorption spectra were meticulously recorded using a Systonic spectrophotometer (Model S-921) within a wavelength range of 200 to 600 nm while maintaining a stable room temperature to ensure accurate readings.

To determine the elemental composition of the AgNPs, Energy-dispersive X-ray spectroscopy (EDX) was performed utilizing a Scanning electron microscope (FE-SEM, OXFORD EDS LM 2). This analysis provided detailed insights into the elemental makeup of the nanoparticles. Further examination of morphology was conducted with a high-resolution JEOL JSM-7610F FE-SEM, allowing a comprehensive view of the nanoparticle structure.

The crystallinity and phase information of the AgNPs were assessed through X-ray diffraction (XRD) using a Bruker AXS D8 advanced X-ray diffractometer, which employed $\text{Cu K}\alpha$ radiation ($\lambda = 1.5418 \text{ \AA}$). This technique provided invaluable data on the crystallographic characteristics of the synthesized nanoparticles. Finally, the thermal stability and properties of the samples were evaluated using a Perkin Elmer thermogravimetric analyzer. This assessment was carried out under a nitrogen atmosphere at a consistent heating rate of $30^\circ\text{C}/\text{min}$, enabling a thorough understanding of the thermal behavior of the AgNPs.

Results and Discussion

In our initial color experiments, we discovered an intriguing pattern: the samples that transformed into a notable pink hue after the introduction of hydrochloric acid (HCl) were classified as adulterated. This finding is effectively presented in the accompanying fig. 4. Out of the four samples analyzed, only 2, 3 and 4, emerged as adulterated, highlighting a significant distinction in their chemical reaction to the acid compared to the others.

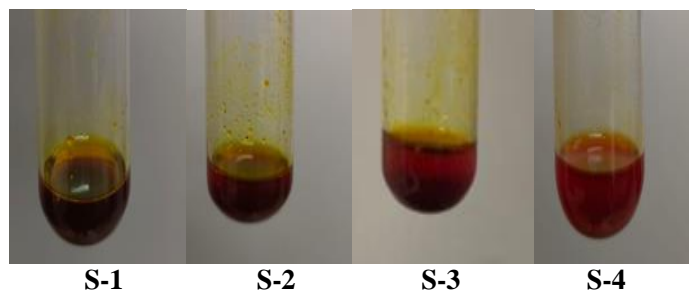


Fig. 4: Chemical analysis of adulteration in different samples of turmeric

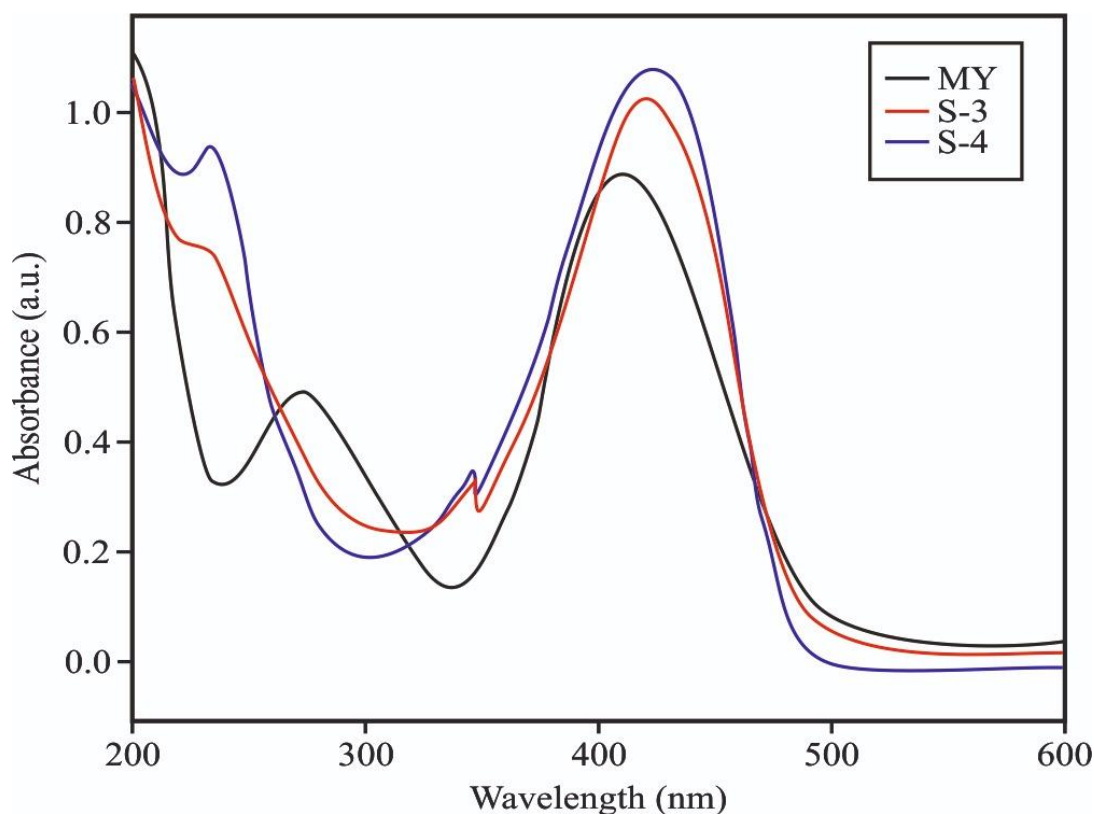


Fig. 5: UV-visible absorption spectra of metanil yellow and the adulterated turmeric samples

In the context of UV-Vis absorption analysis, two prominent high-energy absorption bands are detected at 205 nm and 270 nm wavelengths in the uncontaminated sample. Furthermore, the $n-\pi^*$ transition occurring at 413 nm plays a critical role, as it is responsible for the vibrant color that we see in the turmeric²⁷. In contrast, the adulterated turmeric samples displayed three distinct bands: two high-energy bands located around 205 nm and 215 nm and a broad band near 420 nm, as depicted in fig. 5. The HCl test and UV-Vis absorption analysis results clearly indicate that samples 3 and 4 are contaminated with the adulterant, identified as MY, confirming the presence of impurities in these samples.

Figure 6 presents a detailed view of the absorption spectra measured for glycine-capped silver nanoparticles (Gly-AgNPs). The spectra reveal a strong absorption peak within the 400–420 nm range, characteristic of surface plasmon resonance (SPR) specific to silver nanoparticles. This pronounced peak serves as a clear indicator of successful nanoparticle formation. In fig. 7, the X-ray diffraction

(XRD) patterns of the silver nanoparticles are displayed, strikingly illustrating their crystalline nature. The observed peak values align closely with those of metallic silver (JCPDS No. 04-0783), further validating the material's identity. Notably, the AgNPs exhibit four distinct diffraction peaks at 2θ values of 38.2°, 44.1°, 64.4° and 77.3°. These peaks correspond to the (111), (200), (220) and (311) Bragg reflections of crystalline AgNPs respectively as identified by Shankar et al¹⁹.

A fascinating observation is that the growth of the (111) plane is more prominent than that of the other crystal planes, suggesting a preferred orientation in growth along the (111) direction, as supported by findings in previous studies²⁰. Furthermore, the literature highlights that the strong (111) reflection is recognized as the basal or top crystal plane of silver nanoparticles⁶. This indicates that glycine molecules tend to adsorb onto this specific plane of silver. Supporting this notion, research has shown that the (111) plane possesses the lowest surface energy, which

facilitates the stabilization of silver particles through the adsorption of capping agents³⁰. The average size of the silver nanoparticles, estimated using the Scherrer equation and based on the full width at half maximum (FWHM)⁴ of the prominent (111) reflection, is approximately 16 nm.

Additionally, thermogravimetric analysis (TGA) further corroborates the adsorption of glycine onto the silver nanoparticles, reinforcing the integrity and stability of this unique nanomaterial.

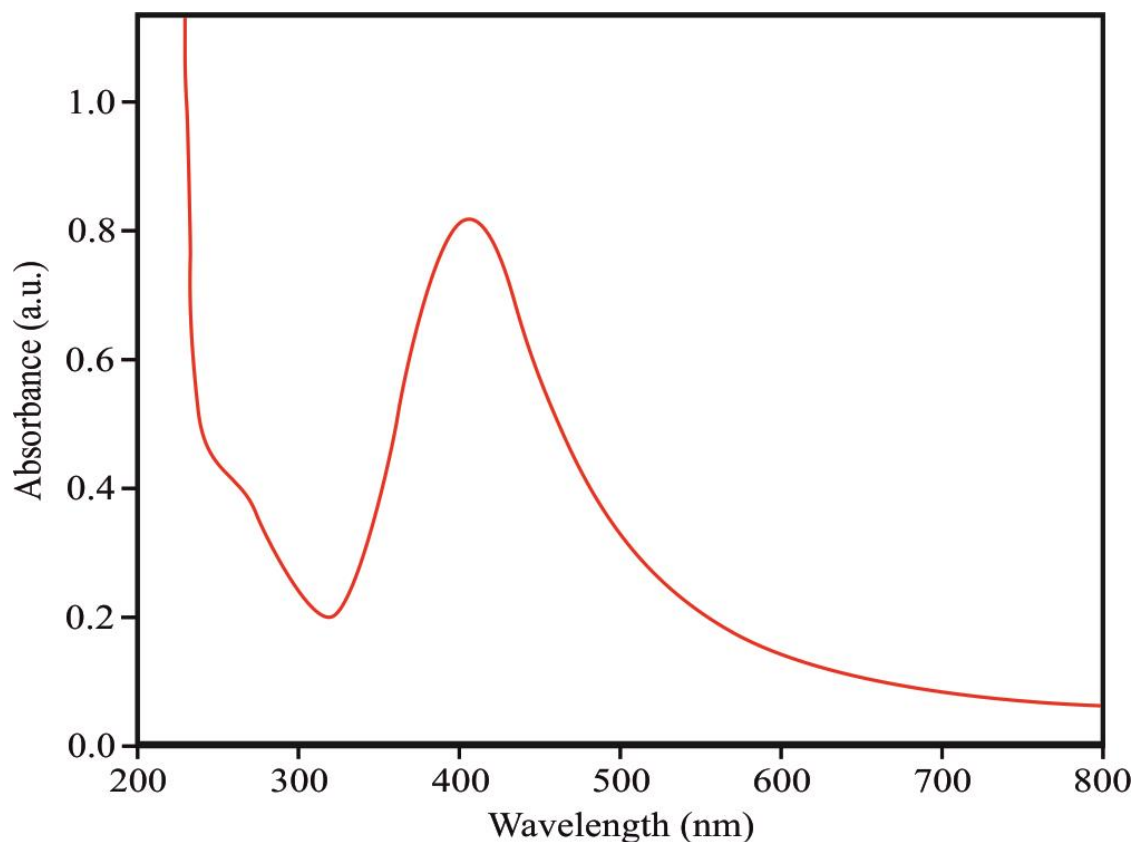


Fig. 6: UV-visible absorption spectra of Gly-AgNPs

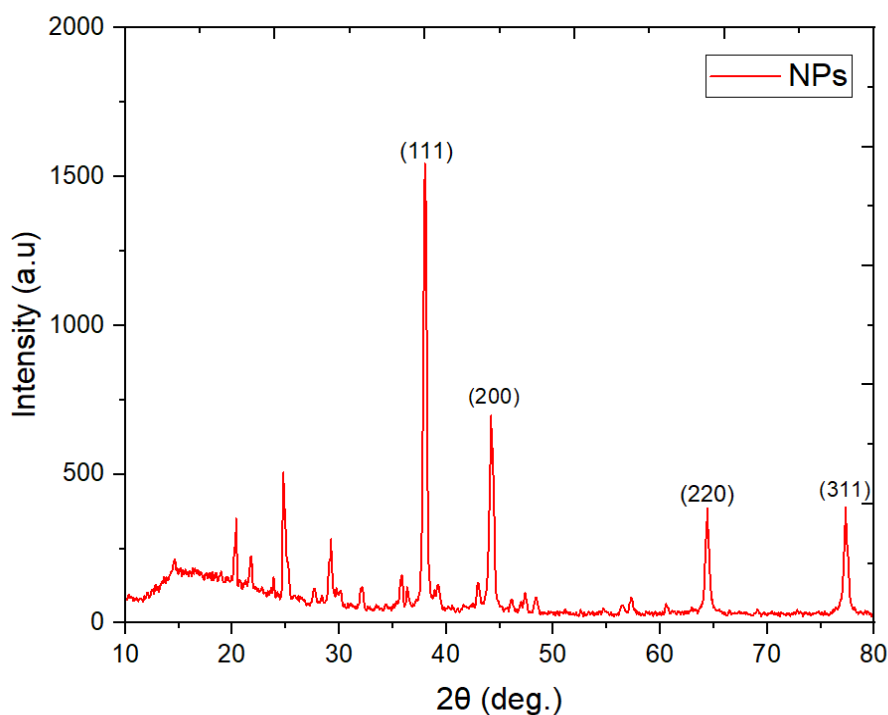


Fig. 7: XRD analysis of Gly-AgNPs

The surface morphology of the synthesized silver nanoparticles (AgNPs) was thoroughly investigated using Scanning electron microscopy (SEM), as illustrated in fig. 8. The SEM micrograph depicting the pure amino acid-capped AgNPs (Fig.7A) reveals a distinct cubic structure that suggests a uniform and well-defined shape. Accompanying this, the energy-dispersive X-ray (EDX) spectra presented in fig. 7B confirm the presence of key elements: silver (Ag), nitrogen (N), carbon (C) and oxygen (O). Notably, the absence of any impurities in the spectra further validates the successful formation of glycine-capped silver nanoparticles (Gly-AgNPs).

To gain deeper insights into the interaction between glycine molecules and the silver nanoparticles, thermogravimetric analysis (TGA) was performed. Fig. 9 illustrates the TGA profiles for the Gly-capped silver nanoparticles, revealing a significant two-step decomposition process. The first stage of mass loss initiates after reaching a temperature of 150 °C, indicating the breakdown of glycine molecules. This weight loss continues until 800 °C, highlighting the stability of the nanoparticle structure while emphasizing the gradual release and decomposition of the adsorbed glycine, thereby providing valuable information about the thermal properties and interactions of the glycine-capped silver nanoparticles.

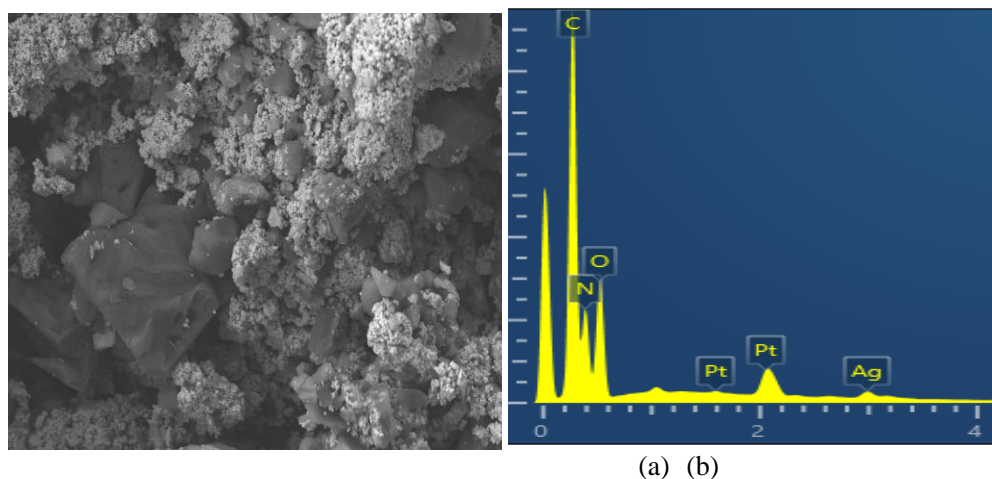


Fig. 8: Gly-AgNPs (a) SEM and (b) EDX

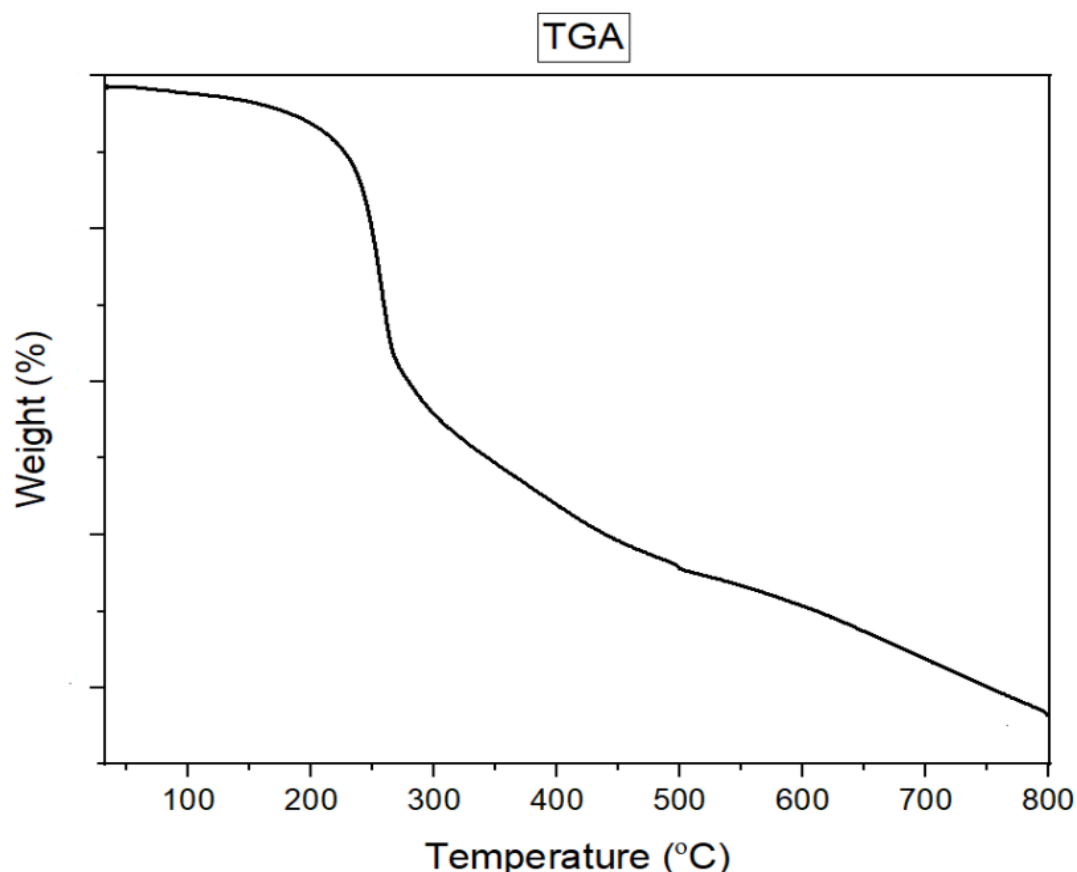


Fig. 9: TGA profile of Gly-AgNPs

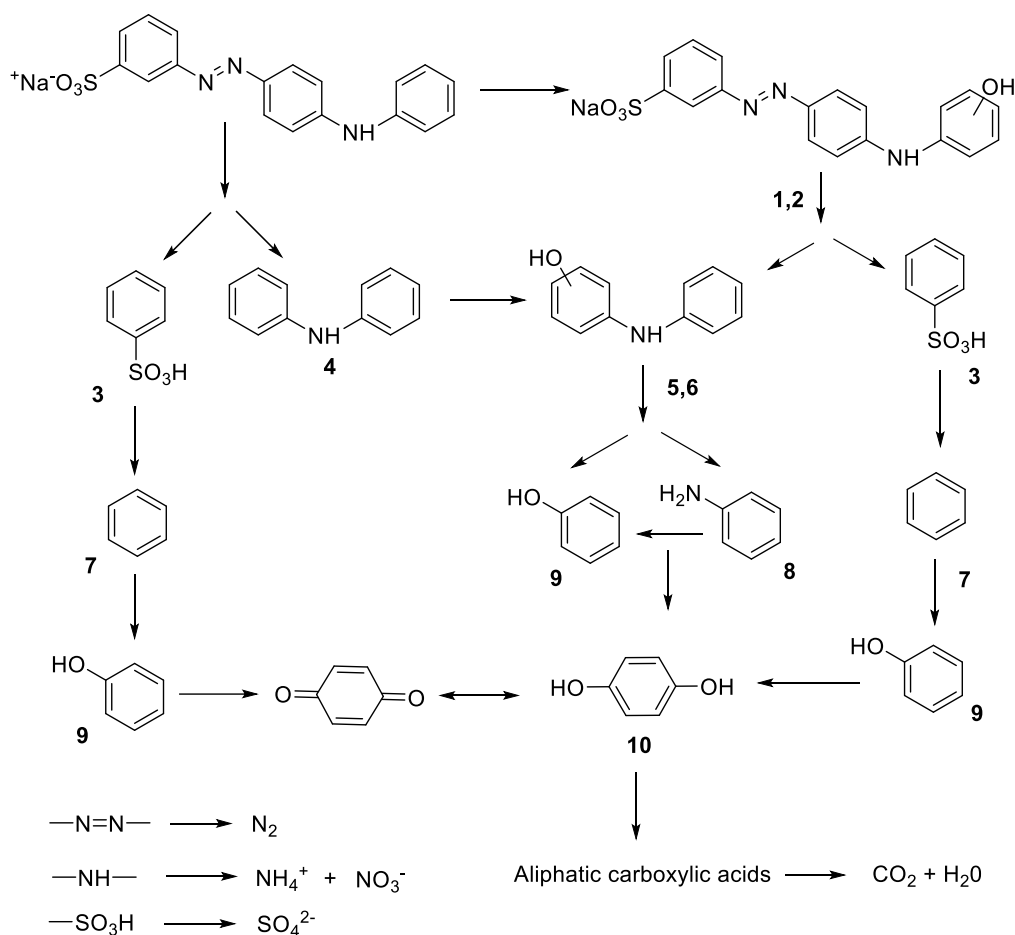


Fig. 10: Schematic representation of the degradation mechanism of metanil yellow dye²⁶

The analytical characterization techniques provide compelling evidence that amino acids can effectively serve as capping agents to inhibit the aggregation of silver nanoparticles (AgNPs). Specifically, amino acids play a crucial role by: (i) preventing the clustering of AgNPs, (ii) enhancing their water solubility, (iii) facilitating the formation of well-dispersed cubic nanoparticles with an approximate size of 16 nanometers, (iv) selectively interacting with silver at its surface and (v) imparting remarkable stability to the AgNPs. This multifaceted approach underscores amino acids' potential in stabilizing and functionalizing silver nanoparticles for various applications.

Photocatalysis: After the azo group (-N=N-) broke down, MY became decolorized and underwent full mineralization²⁶. Several organic intermediates were created when metanil yellow underwent photocatalytic oxidation. By considering its degradation mechanism, dye degradation can be researched. Based on the identification results, a thorough reaction pathway is suggested, as shown schematically in fig. 10. The following are the steps of degradation that are most likely involved. In this pathway, products formed in each step are as the primary hydroxylated by-products (1, 2), benzene sulfonic acid (3), diphenylamine (4), hydroxyl-diphenyl amine ortho isomers

(5) and para- (6), benzene (7), aniline (8) and phenol (9) and hydroquinone (10)

Metanil yellow is an aromatic dye used for industrial applications, such as dyeing wool, nylon, silk, paper, ink, aluminum and detergent. But the adulterated turmeric contains some amount of MY. Research has unveiled that this chemical can lead to severe toxic effects on various bodily systems, even when consumed in minimal doses over extended periods^{7,14}. When this adulterated turmeric was treated for a particular period with Gly-AgNPs, the color of the reaction mixture decreased gradually from orange-yellow to light-yellow because of the photocatalytic degradation reaction of AgNPs under sunlight. The absorption spectra of the reaction mixtures confirmed these results. The absorption band for MB dye is observed at 420 nm due to the $n\text{-}\pi^*$ transition of electrons.

The photocatalytic degradation of the reaction mixture was clear from the decreasing absorption intensity as time passed under sunlight. This decrease in absorption intensity is due to the surface plasma resonance of AgNPs. In the present work, degradation was followed up to 2 hours and a noticeable decrease in the peak intensity of metanil yellow (MY) was observed (Fig. 11).

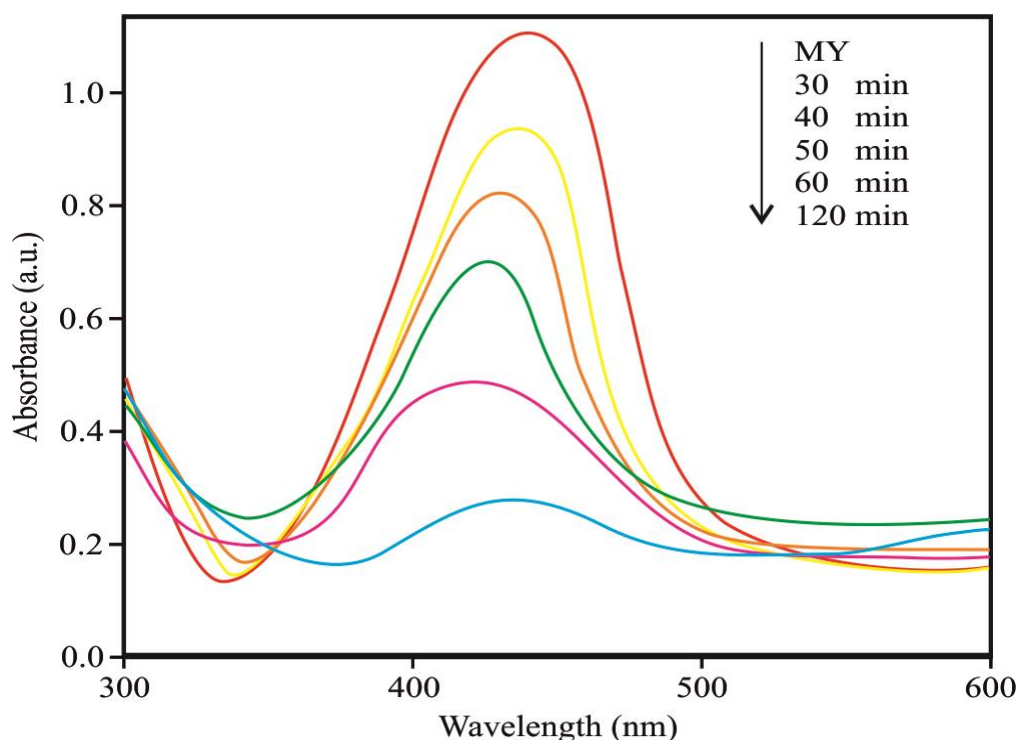


Fig. 11: UV-Vis spectra for photocatalytic degradation of metanil yellow

So, it is clear from the results that synthesized Gly-AgNPs are good efficient photocatalytic agents for the degradation of metanil yellow dye under sunlight. This method can be used to purify adulterated turmeric.

Conclusion

Turmeric, widely recognized as *Haridra*, is more than just a popular spice; it is revered in many cultures' culinary traditions and medicinal practices worldwide. Its rich, golden hue and aromatic profile make it a staple in countless recipes, while its health benefits have been celebrated for centuries. However, the pervasive issue of food adulteration poses a serious threat, even to this essential spice. Turmeric is often targeted for fraudulent practices, particularly by adding harmful substances such as metanil yellow dye (MY). This situation raises critical health concerns and calls for urgent solutions. In response to this challenge, our research focused on the innovative synthesis of silver nanoparticles (Gly-AgNPs), which are capped with glycine, a simple amino acid. These nanoparticles were subjected to a rigorous characterization process utilizing State-of-the-Art analytical techniques. We employed X-ray diffraction (XRD) to determine the crystalline structure, Scanning electron microscopy (SEM) to visualize their surface morphology, Ultraviolet-Visible (UV) spectroscopy to study their optical properties and Energy dispersive X-ray (EDX) analysis to assess their elemental composition. Our study harnessed the remarkable photocatalytic properties of these glycine-capped silver nanoparticles to target metanil yellow dye, a prevalent adulterant found in turmeric samples.

Throughout our experiments, we meticulously optimized various parameters including the concentrations of both the

dye and the nanoparticles and the reaction solutions' temperature and pH levels. The results of our investigation were striking: the glycine-capped silver nanoparticles emerged as highly effective catalysts, achieving a remarkable 89% reduction in the concentration of the metanil yellow dye. This substantial reduction highlights the potential of Gly-AgNPs as efficient agents in the degradation of toxic dyes and suggests their promising applicability in various environmental and industrial contexts. Our research shows the importance of developing strategies to combat food adulteration and to protect public health while paving the way for future innovations in nanotechnology and photocatalysis.

Acknowledgement

The authors express gratitude to the administration of GLA University in Mathura, India, for permitting them to utilize the University's facilities to conduct this research.

References

1. Ahmed M.A., Messih M.F.A., El-Sherbeny E.F., El-Hafez S.F. and Khalifa A.M.M., Synthesis of metallic silver nanoparticles decorated mesoporous SnO₂ for removal of methylene blue dye by coupling adsorption and photocatalytic processes, *J. Photochem. Photobiol. A Chem.*, **346**, 77-88 (2017)
2. Alves S.P., Brum D.M., de Andrade É.C.B. and Netto A.D.P., Determination of synthetic dyes in selected foodstuffs by high performance liquid chromatography with UV-DAD detection, *Food Chem.*, **107**(1), 489-496 (2008)
3. Baruah D., Goswami M., Yadav R.N.S., Yadav A. and Das A.M., Biogenic synthesis of gold nanoparticles and their application in photocatalytic degradation of toxic dyes, *J. Photochem. Photobiol. B Biol.*, **186**, 51-58 (2018)

4. Birks L.S. and Friedman H., Particle size determination from X-ray line broadening, *J. Appl. Phys.*, **17(8)**, 687-692 (1946)
5. Chandila J. and Puri D., A comparative study on consumer perception towards packaged spices among rural and urban women, *Int J Heal. Sci Res*, **9(8)**, 399-405 (2019)
6. Chen S. and Carroll D.L., Synthesis and characterization of truncated triangular silver nanoplates, *Nano Lett.*, **2(9)**, 1003-1007 (2002)
7. Choi H., Risk assessment of daily intakes of artificial colour additives in food commonly consumed in Korea, *J. Food Nutr. Res.*, **51(1)**, 13-22 (2012)
8. Deng Y. and Zhao R., Advanced oxidation processes (AOPs) in wastewater treatment, *Curr. Pollut. Reports*, **1**, 167-176 (2015)
9. Downham A. and Collins P., Colouring our foods in the last and next millennium, *Int. J. food Sci. & Technol.*, **35(1)**, 5-22 (2000)
10. Huynh Phuoc, Nguyen Thi Thuong Huyen and Thai Ke Quan, Computational assessment of spike-hACE2 binding affinity in omicron subvariant BA.2.86, *Res. J. Biotech.*, **19(2)**, 1-13 (2024)
11. Khanna S.K., Toxicity, carcinogenic potential and clinicoepidemiological studies on dyes and dye intermediates, *J. Sci. Ind. Res.*, **28(8)**, 965-974 (1991)
12. Leong K.H., Abd Aziz A., Sim L.C., Saravanan P., Jang M. and Bahnemann D., Mechanistic insights into plasmonic photocatalysts in utilizing visible light, *Beilstein J. Nanotechnol.*, **9(1)**, 628-648 (2018)
13. Nawaz M.S. and Ahsan M., Comparison of physico-chemical, advanced oxidation and biological techniques for the textile wastewater treatment, *Alexandria Eng. J.*, **53(3)**, 717-722 (2014)
14. Rajapaksha G.K.M., Wansapala M.A.J. and Silva A.B.G., Detection of synthetic colours in selected foods & beverages available in Colombo district, Sri Lanka, *Int. J. Sci. Res*, **6**, 801-808 (2017)
15. Reverberi A.P., Kuznetsov N.T., Meshalkin V.P., Salerno M. and Fabiano B., Systematical analysis of chemical methods in metal nanoparticles synthesis, *Theor. Found. Chem. Eng.*, **50**, 59-66, (2016)
16. Reyes F.G.R., Valim M. and Vercesi A.E., Effect of organic synthetic food colours on mitochondrial respiration, *Food Addit. & Contam.*, **13(1)**, 5-11 (1996)
17. Sarkar B., Xi Y., Megharaj M., Krishnamurti G.S.R., Rajarathnam D. and Naidu R., Remediation of hexavalent chromium through adsorption by bentonite based Arquad®2HT-75 organoclay, *J. Hazard Mater.*, **183(1-3)**, 87-97, (2010)
18. Sarkar R. and Ghosh A.R., Toxicological effect of Metanil Yellow on the testis of albino rat, *Int. J. Basic Appl. Med. Sci.*, **2(2)**, 40-42 (2012)
19. Shankar S., Chorachoo J., Jaiswal L. and Voravuthikunchai S.P., Effect of reducing agent concentrations and temperature on characteristics and antimicrobial activity of silver nanoparticles, *Mater. Lett.*, **137**, 160-163 (2014)
20. Shankar S., Prasad R., Selvakannan P.R., Jaiswal L. and Laxman R.S., Green synthesis of silver nanoribbons from waste X-ray films using alkaline protease, *Mater. Express*, **5(2)**, 165-170 (2015)
21. Sharma R., Current Understanding and Prospects of Silver Nanoparticles-Based Biosensor, *Nano Life*, **13(04)**, 2330007 (2023)
22. Sharma R., Nanotechnology: pros and cons in food quality, *Nano Life*, **12(01)**, 2230001 (2022)
23. Sharma R., Synthesis of Terminalia bellirica fruit extract mediated silver nanoparticles and application in photocatalytic degradation of wastewater from textile industries, *Mater. Today Proc.*, **44**, 1995-1998 (2021)
24. Singh J., Dutta T., Kim K.H., Rawat M., Samddar P. and Kumar P., 'Green' synthesis of metals and their oxide nanoparticles: applications for environmental remediation, *J. Nanobiotechnology*, **16**, 1-24 (2018)
25. Singh K. and Arora S., Removal of synthetic textile dyes from wastewaters: a critical review on present treatment technologies, *Crit. Rev. Environ. Sci. Technol.*, **41(9)**, 807-878 (2011)
26. Sleiman M., Vildoza D., Ferronato C. and Chovelon J.M., Photocatalytic degradation of azo dye Metanil Yellow: optimization and kinetic modeling using a chemometric approach, *Appl. Catal. B Environ.*, **77(1-2)**, 1-11 (2007)
27. Verma A., Saha S. and Bhat S.K., Detection of Nonpermitted Food Color Metanil Yellow in Turmeric: A Threat to the Public Health and Ayurvedic Drug Industry, *J. Ayurveda*, **16(2)**, 134-139 (2022)
28. Vieira G.B., José H.J., Peterson M., Baldissarelli V.Z., Alvarez P. and Moreira R. de F.P.M., CeO₂/TiO₂ nanostructures enhance adsorption and photocatalytic degradation of organic compounds in aqueous suspension, *J. Photochem. Photobiol. A Chem.*, **353**, 325-336 (2018)
29. Yadi M. et al, Current developments in green synthesis of metallic nanoparticles using plant extracts: a review, *Artif. Cells, Nanomedicine, Biotechnol.*, **46(Sup 3)**, 336-343 (2018)
30. Yang J., Lu L., Wang H., Shi W. and Zhang H., Glycyl glycine templating synthesis of single-crystal silver nanoplates, *Cryst. Growth & Des.*, **6(9)**, 2155-2158 (2006)
31. Zhang X.F., Liu Z.G., Shen W. and Gurunathan S., Silver nanoparticles: Synthesis, characterization, properties, applications and therapeutic approaches, *Int. J. Mol. Sci.*, **17(9)**, 1534 (2016).

(Received 13th February 2025, accepted 15th April 2025)